

## Supporting Information

### Tumour-homing chimeric polypeptide-conjugated polypyrrole nanoparticles for imaging-guided synergistic photothermal and chemical therapy of cancer

Mengmeng Sun,<sup>1</sup> Jianwen Guo,<sup>1</sup> Hanjun Hao,<sup>1</sup> Tong Tong,<sup>2</sup> Kun Wang<sup>2</sup> and Weiping Gao<sup>1\*</sup>

<sup>1</sup> Department of Biomedical Engineering, School of Medicine, Tsinghua University, Beijing 100084, China

<sup>2</sup> Key Laboratory of Molecular Imaging, the State Key Laboratory of Management and Control for Complex Systems, Institute of Automation, Chinese Academy of Sciences, Beijing, 100190, China.

\*Corresponding author: E-mail: gaoweiping@tsinghua.edu.cn

#### Supplementary Figure1-24, Table 1-3

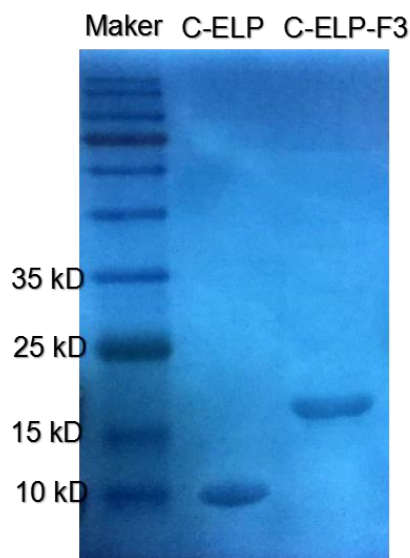


**Figure S1.** SDS-PAGE analyses of C-ELP (lane 2, 13.6 kDa) and C-ELP-F3 (lane 3, 16.9 kDa) purification by inverse transition cycling (ITC). Lane 1: molecular mass marker.

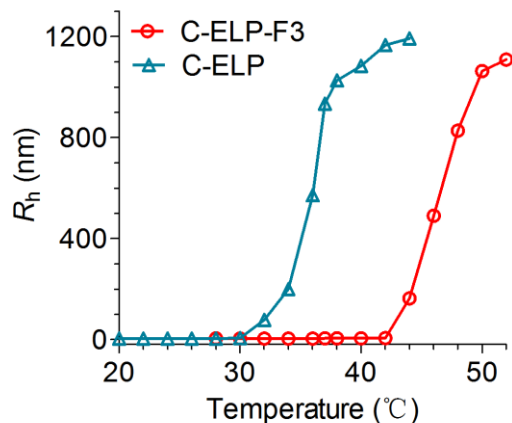


**Figure S2.** The temperature dependence of hydrodynamic radius ( $R_h$ ) of C-ELP and C-ELP-F3 at the same concentration of 25  $\mu\text{M}$  in PBS.

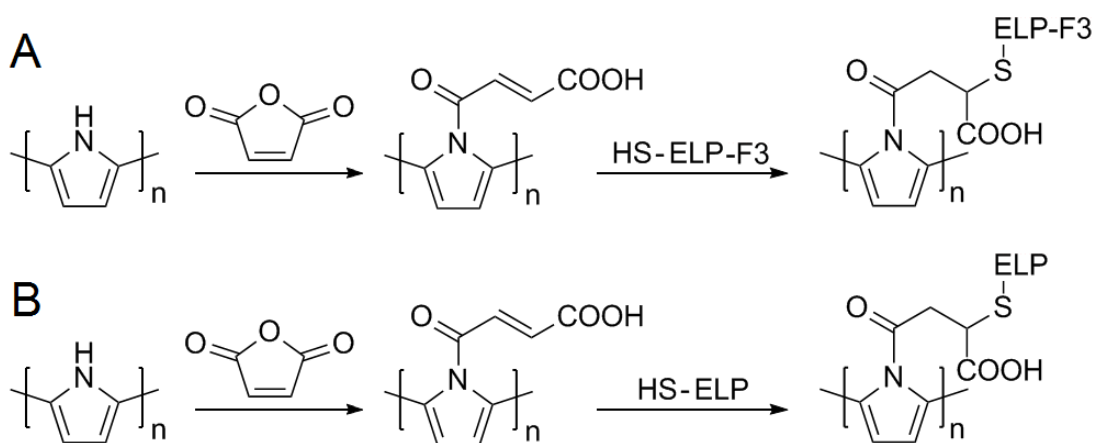


**Figure S3.** Schematic illustration of the synthesis of PPy-ELP-F3 (A) and PPy-ELP (B) nanoparticles.

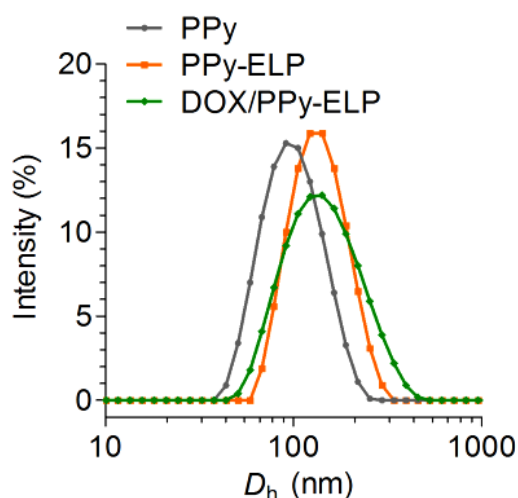


**Figure S4.** DLS profiles of PPy, PPy-ELP and DOX/PPy-ELP.  $D_h$  denotes hydrodynamic diameter.

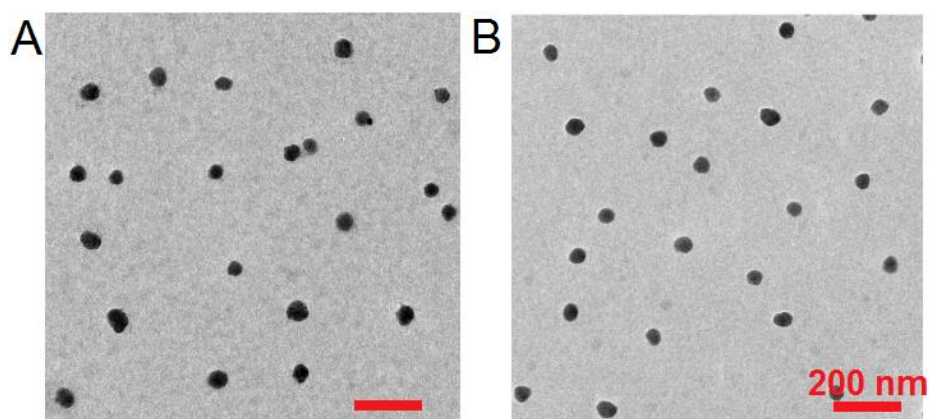


**Figure S5.** The TEM images of PPy-ELP (A) and DOX/PPy-ELP (B) at 25 °C

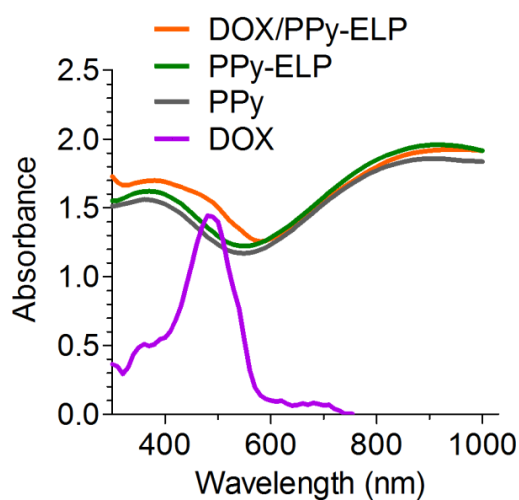


**Figure S6.** The absorption spectra of DOX, PPy, PPy-ELP and DOX/PPy-ELP at the same concentration of PPy in PBS at 25 °C.

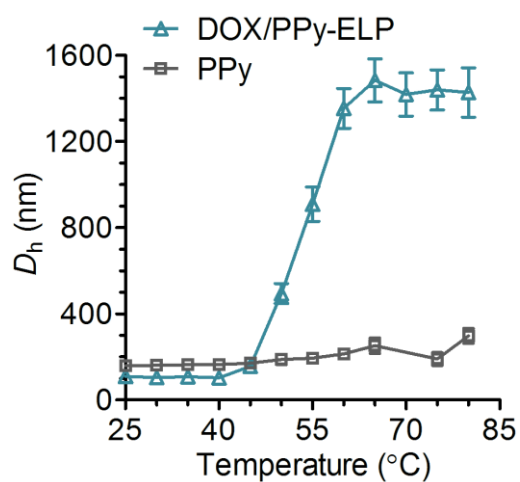


**Figure S7.** The temperature dependence of hydrodynamic diameters ( $D_h$ ) of DOX/PPy-ELP and PPy at the same concentration of PPy (500 mg/L). Error bars are based on standard deviations of triplicated samples.

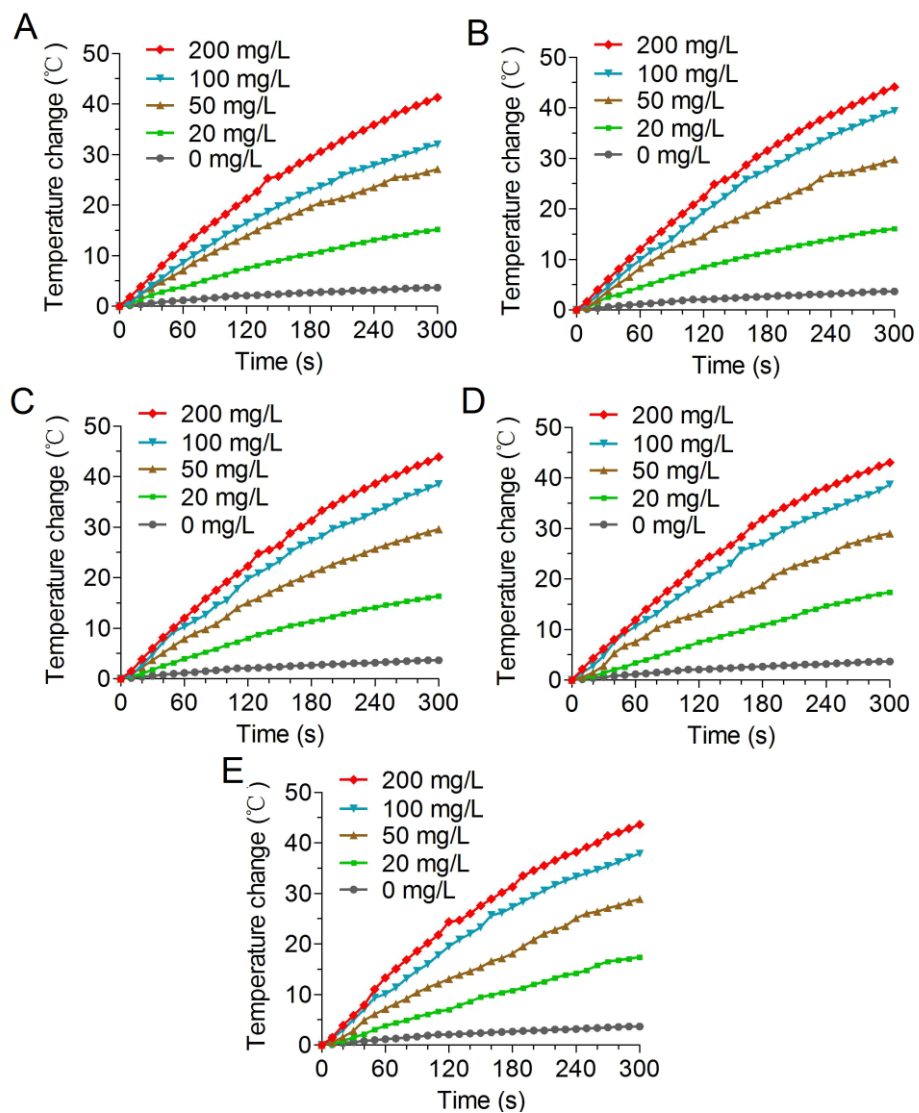


**Figure S8.** Heating curves of PPy (A), PPy-ELP (B), PPy-ELP-F3 (C), DOX/PPy-ELP (D) and DOX/PPy-ELP-F3 (E) samples at different concentrations under 808 nm laser irradiation (1.5 W/cm<sup>2</sup>, 5 min).

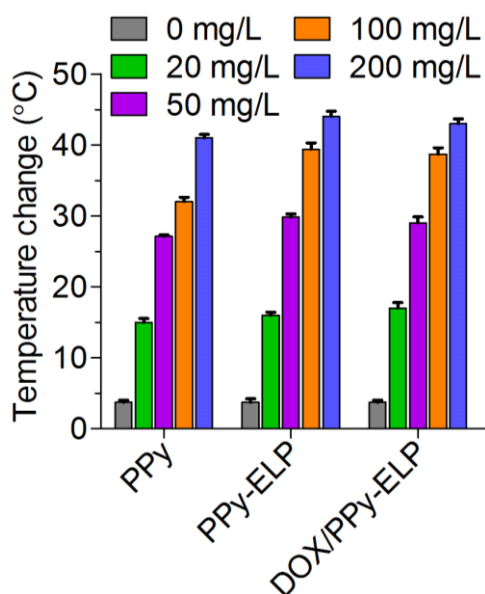


**Figure S9.** The PPy concentration dependence of temperatures of PPy, PPy-ELP and DOX/PPy-ELP solutions exposed to laser irradiation (808 nm, 1.5 W/cm<sup>2</sup>, 5 min). Error bars are based on standard deviations of triplicated samples.

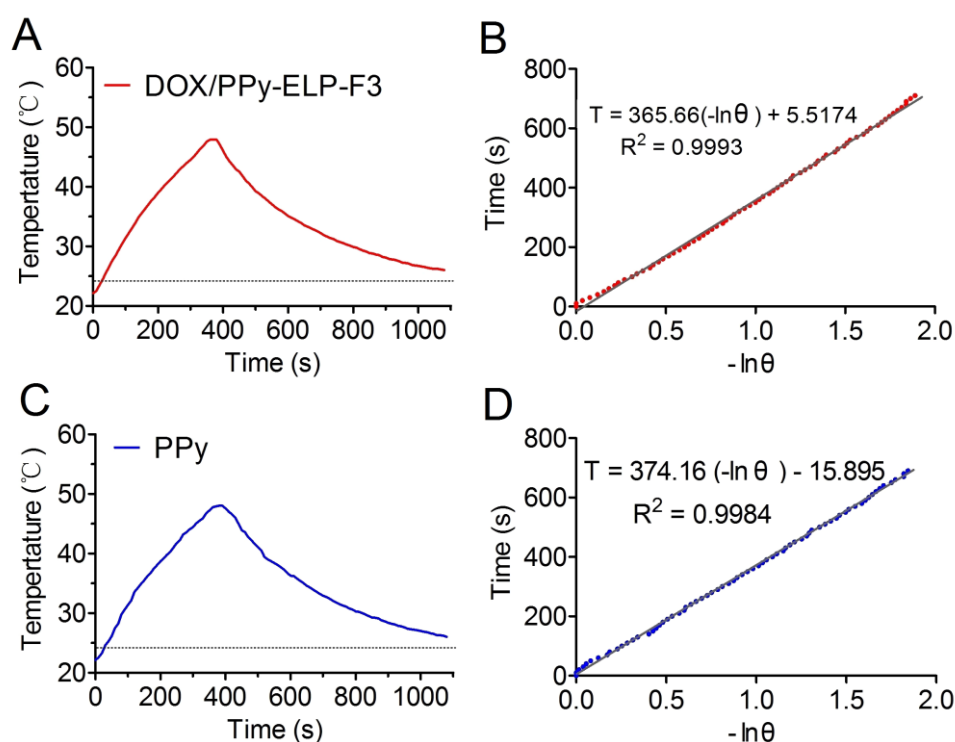


**Figure S10.** Photothermal transfer efficiency of DOX/PPy-ELP-F3 and PPy. (A) The photothermal response of DOX/PPy-ELP-F3 solution (100 mg/L) irradiated under an 808 nm laser at 1.5 W/cm<sup>2</sup> for 370 s, then the laser was turned off. (B) Linear relationship between time and  $\ln\theta$  obtained from the cooling period of (A). (C) The photothermal response of PPy solution (100 mg/L) irradiated under an 808 nm laser at 1.5 W/cm<sup>2</sup> for 380 s, then the laser was turned off. (D) Linear relationship between time and  $\ln\theta$  obtained from the cooling period of (C).

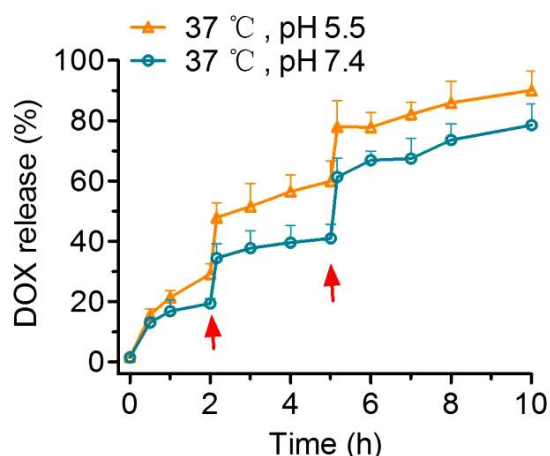


**Figure S11.** NIR-triggered DOX release from DOX/PPy-ELP under different pH. Arrows were the time points when NIR irradiation (808 nm, 1.0 W/cm<sup>2</sup>) was executed for 5 min. Error bars were based on standard deviations of triplicated samples.

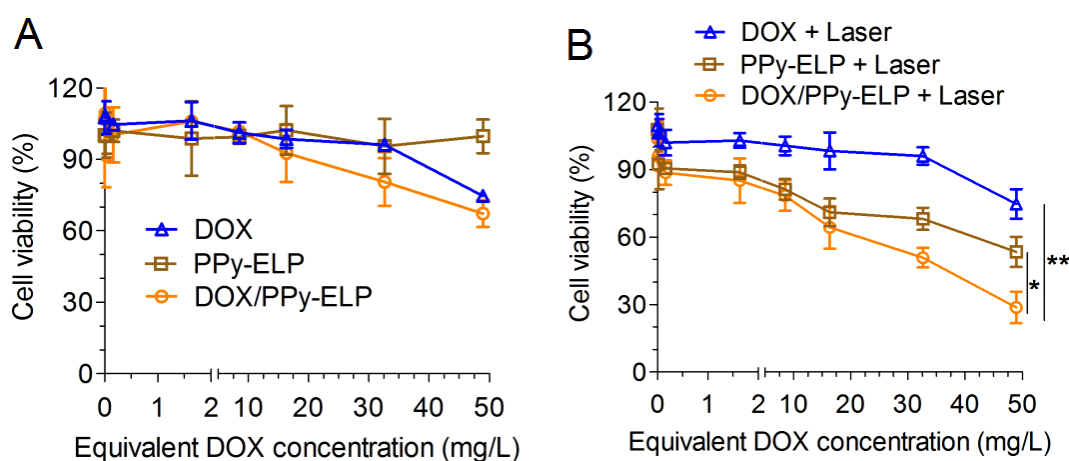


**Figure S12.** Chemical and photothermal cytotoxicity of DOX/PPy-ELP against C8161 melanoma cancer cells. (A) Cell viability of C8161 cells after incubation with different samples for 4 h. (B) Cell viability of C8161 cells after incubation with different samples for 4 h and NIR irradiation (808 nm, 2.5 W/cm<sup>2</sup>, 3 min). PPy-ELP: equivalent to PPy-ELP concentrations in DOX/PPy-ELP solution. Note: the weight ratio of DOX to PPy-ELP was set to be 1:5. \* $P < 0.05$ , \*\* $P < 0.01$ , significant difference for DOX/PPy-ELP plus laser compared with DOX plus laser group.

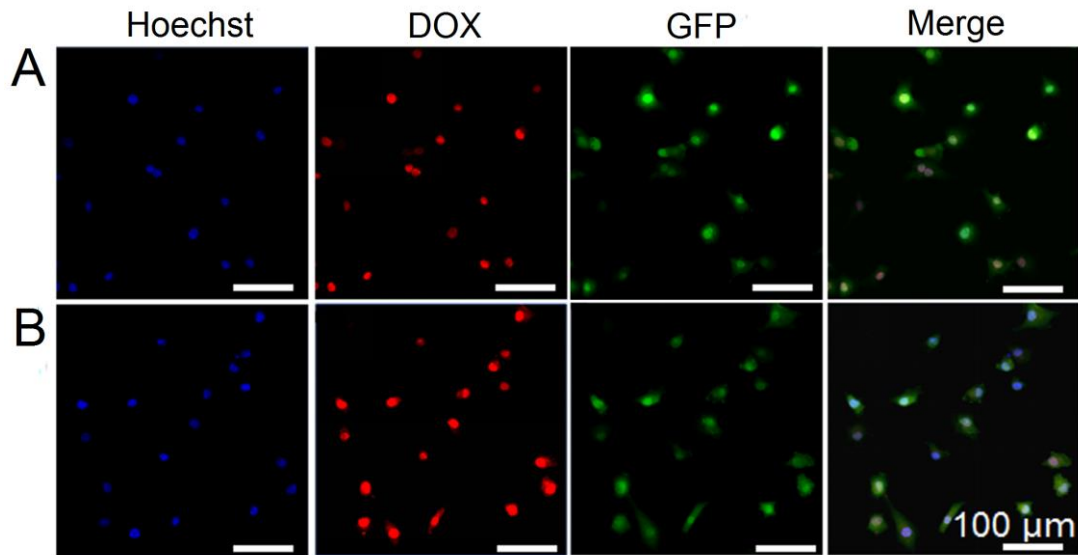


**Figure S13.** Intracellular delivery of DOX into C8161 cells by DOX/PPy-ELP without (A) or with (B) laser irradiation. The cell nucleus was stained with Hoechst 33324 in blue; the cell membrane was green (GFP); DOX/PPy-ELP were shown in red.

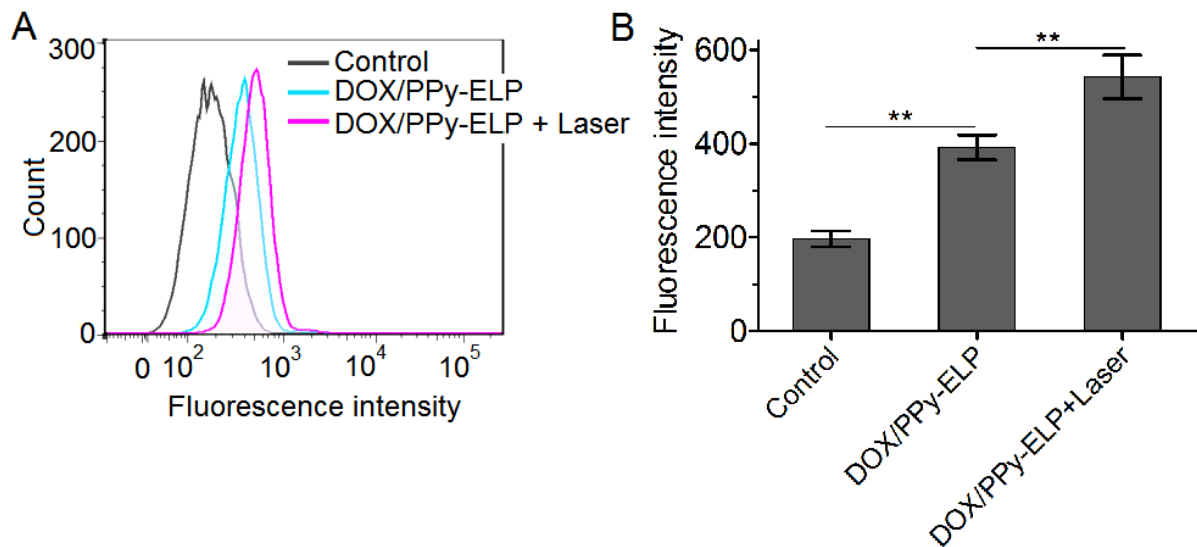


**Figure S14.** The cellular uptake of DOX/PPy-ELP. (A) Fluorescence-activated cell sorting (FACS) analysis of C8161 cell uptake of DOX/PPy-ELP with or without laser irradiation. Laser irradiation: 808 nm, 1.0 W/cm<sup>2</sup>, 2 min. (B) The mean fluorescence intensity of cells calculated from the FACS analysis. \*\* $P < 0.01$ , significant difference for DOX/PPy-ELP plus laser compared with other treatment groups.

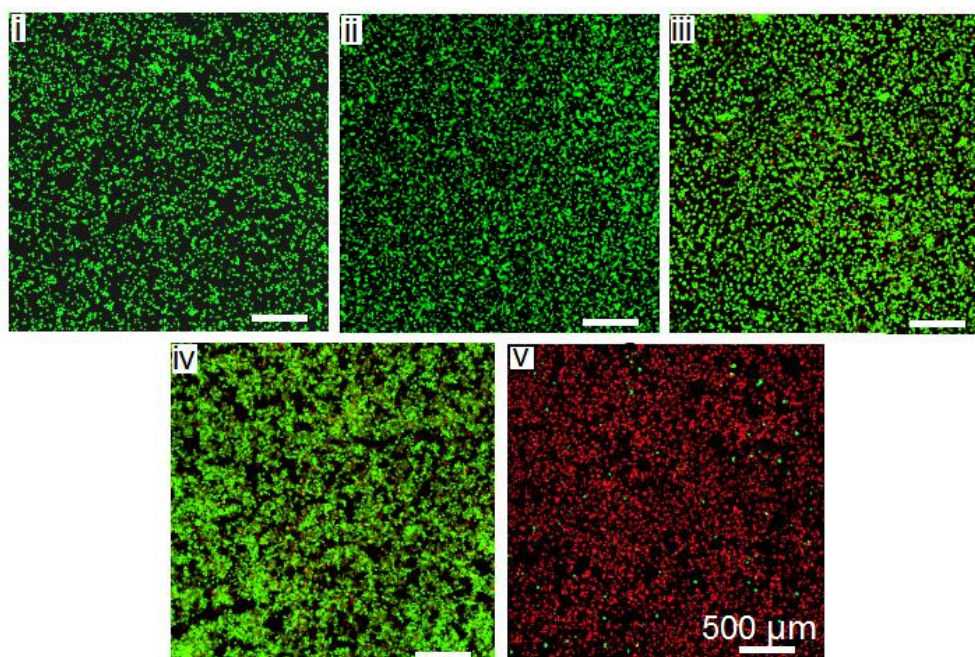


**Figure S15.** Photothermal and chemical destruction of C8161 cells treated with laser only (i), PPy-ELP only (ii), DOX/PPy-ELP only (iii), PPy-ELP plus laser (iv), DOX/PPy-ELP plus laser (v). Laser irradiation: 808 nm, 2.5 W/cm<sup>2</sup>, 3 min.

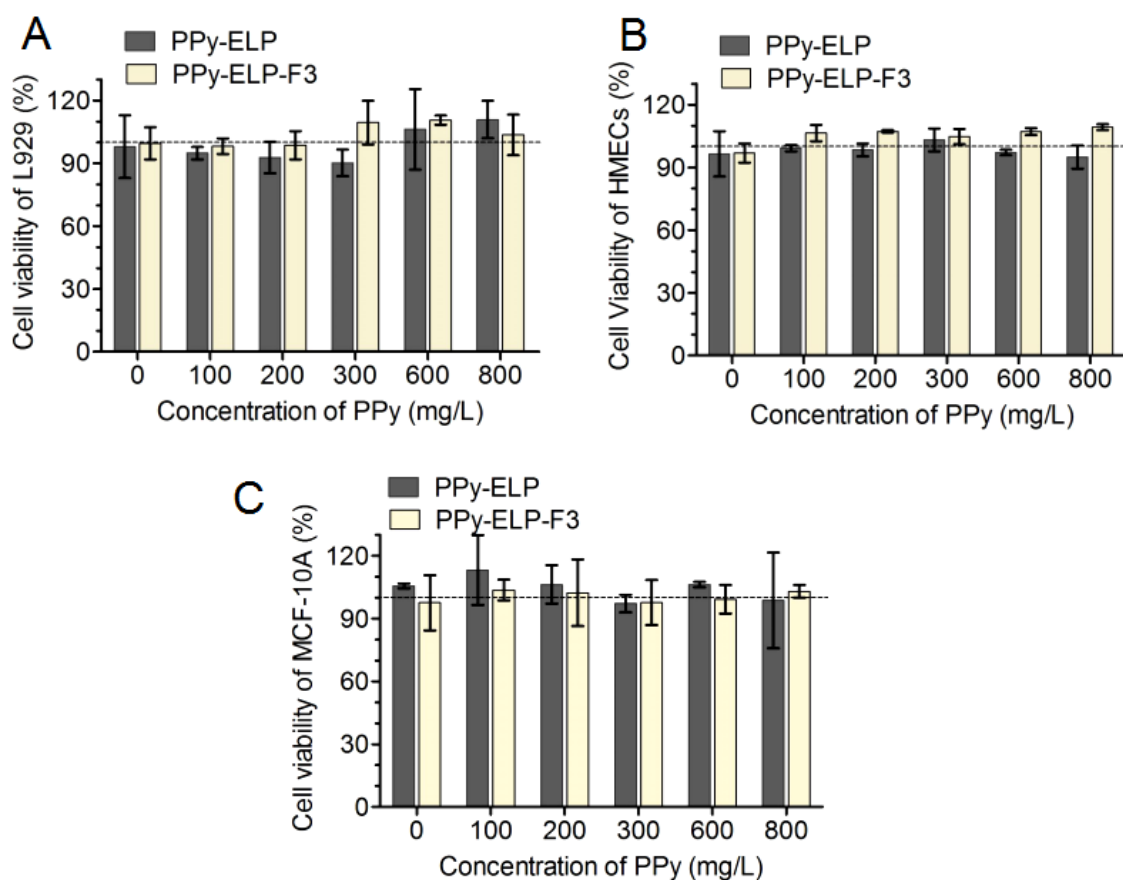


**Figure S16.** Biocompatibility of PPy-ELP-F3. Cell viability of murine fibroblasts L929 cells (A), human microvascular endothelial cells (HMECs) (B) and human mammary epithelial MCF-10A cells (C) after incubation with different concentrations of PPy-ELP-F3 and PPy-ELP for 48 h, as determined by MTS assay.

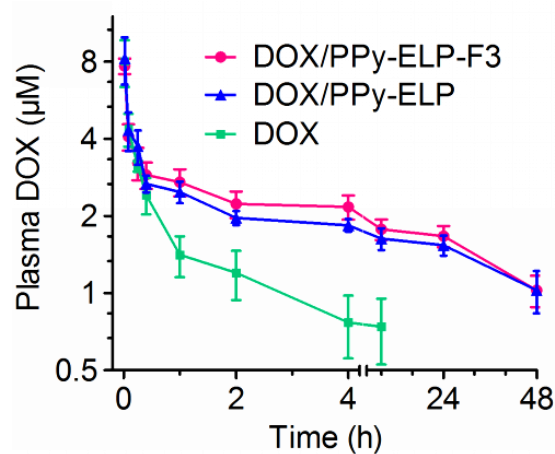


**Figure S17.** *In vivo* pharmacokinetics of DOX/PPy-ELP-F3 and DOX/PPy-ELP compared with free DOX. Plasma DOX concentrations were determined as a function of time post administration (n = 3).

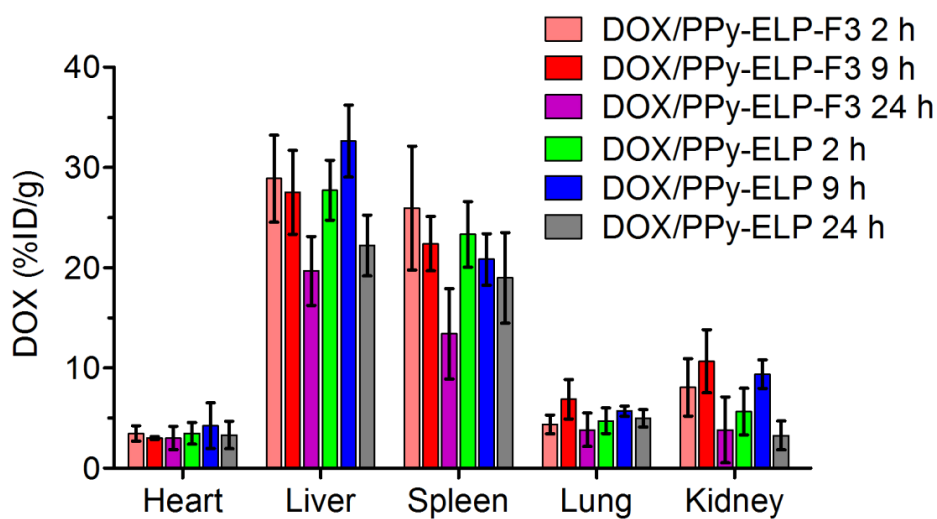


**Figure S18.** Biodistribution of DOX from DOX/PPy-ELP-F3 and DOX/PPy-ELP in tissues at 2 h, 9 h and 24 h post administration. Data are shown as mean  $\pm$  standard deviation (n = 3).

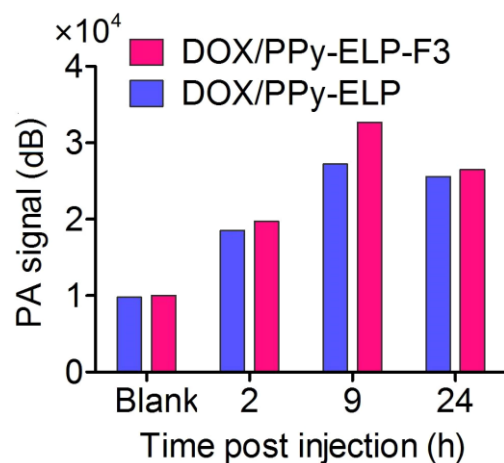


**Figure S19.** Photoacoustic (PA) intensity of tumour tissue treated with DOX/PPy-ELP-F3 and DOX/PPy-ELP as a function of time.

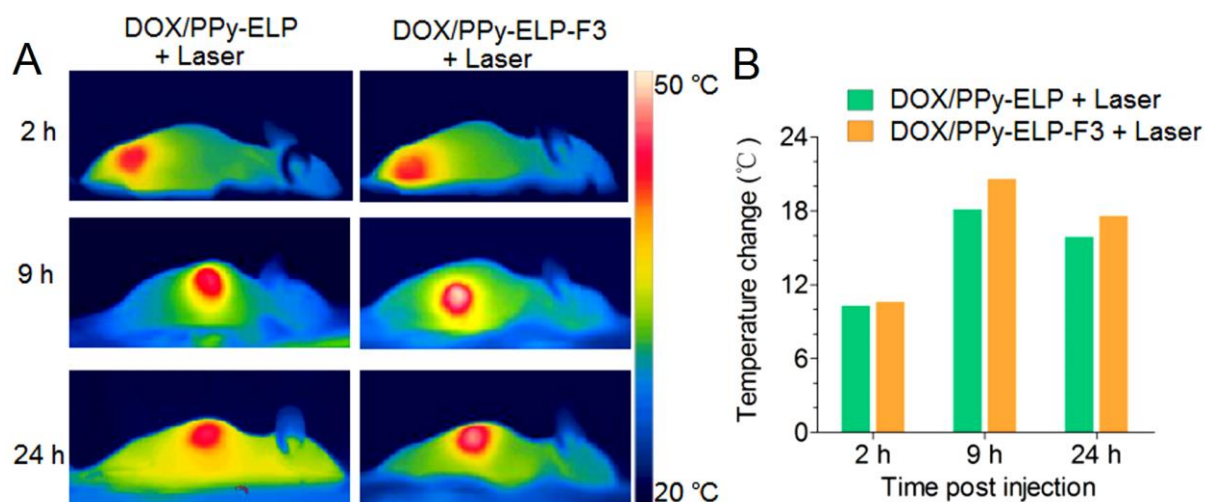


**Figure S20.** (A) IR thermal images of C8161 tumour-bearing mice exposed to an 808 nm laser at a power density of  $1.2 \text{ W/cm}^2$  for 5 min after intravenous injection of DOX/PPy-ELP and DOX/PPy-ELP-F3. (B) The injection time dependence of temperatures of DOX/PPy-ELP and DOX/PPy-ELP-F3 solutions exposed to laser irradiation.

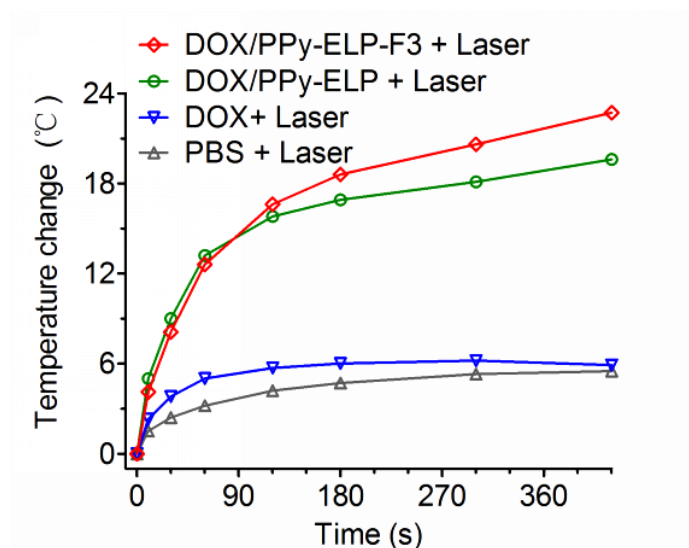


**Figure S21.** Heat curves of tumours upon laser irradiation as a function of irradiation time.

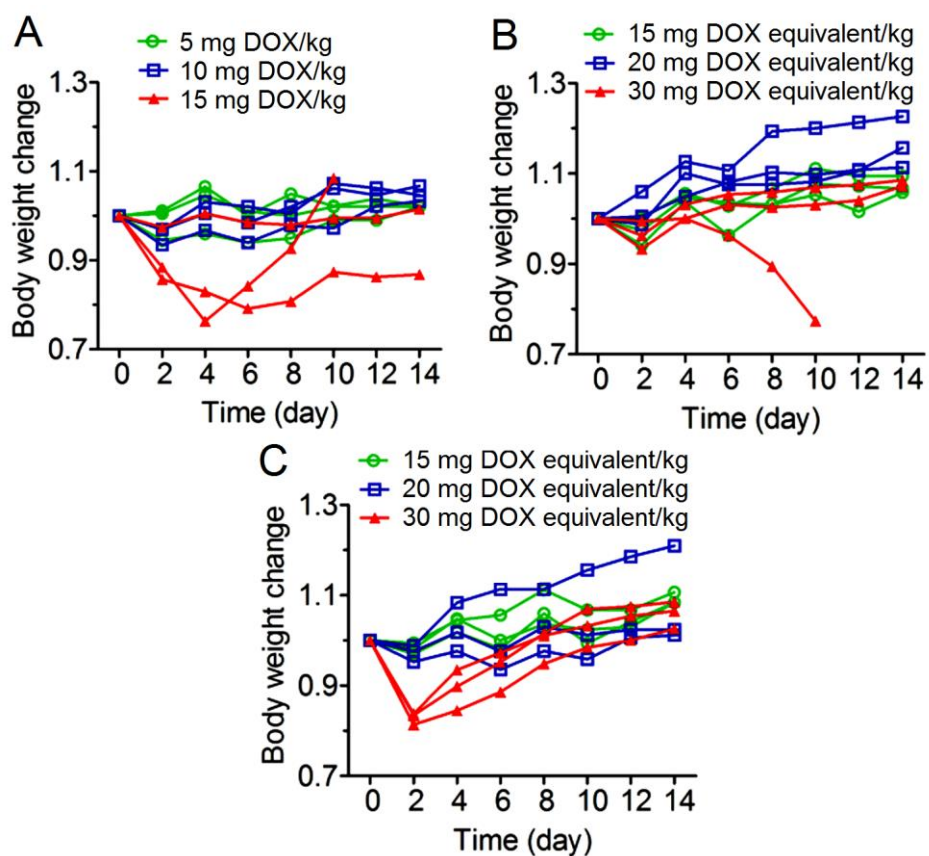


**Figure S22.** The change of body weights of mice treated with free DOX (A), DOX/PPy-ELP (B) and DOX/PPy-ELP-F3 (C) in different DOX concentrations.

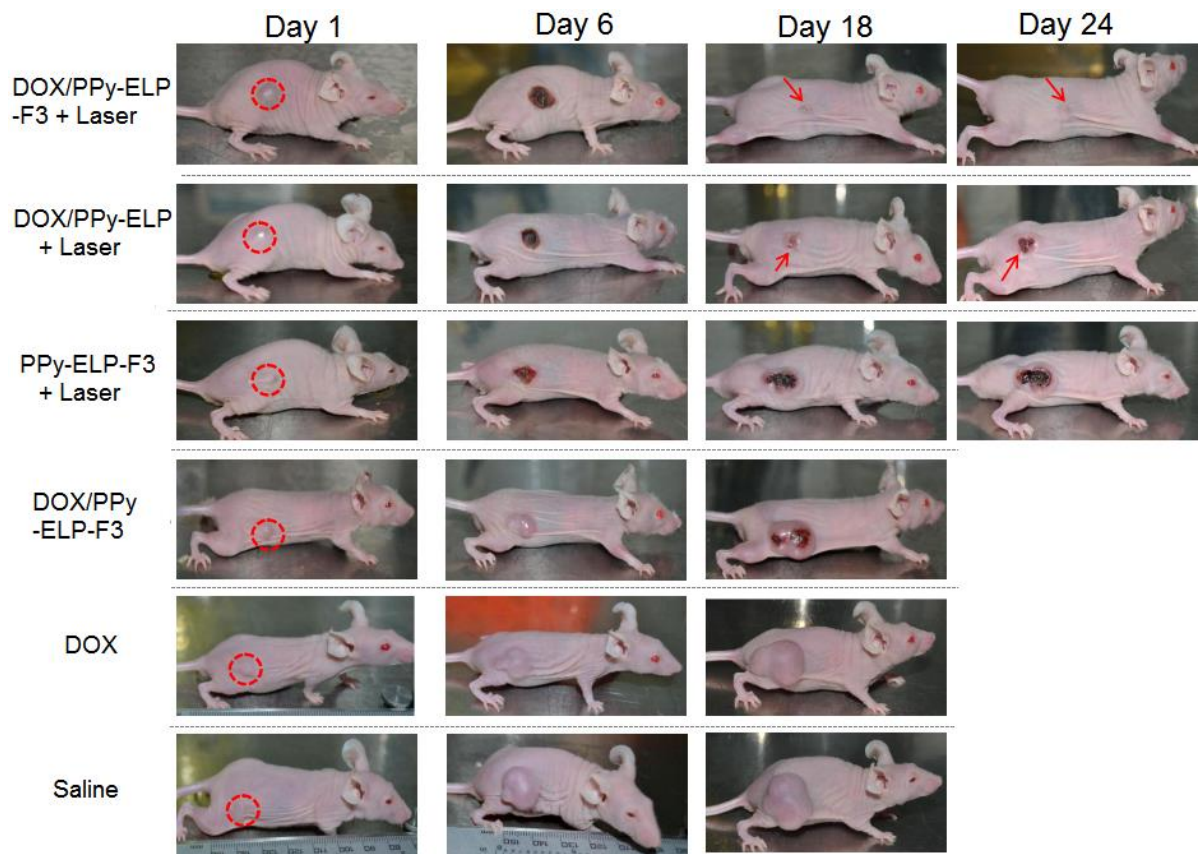


**Figure S23.** Digital pictures of C8161 tumour mice in different groups at 1 day, 6 days, 18 days and 24 days post treatment.

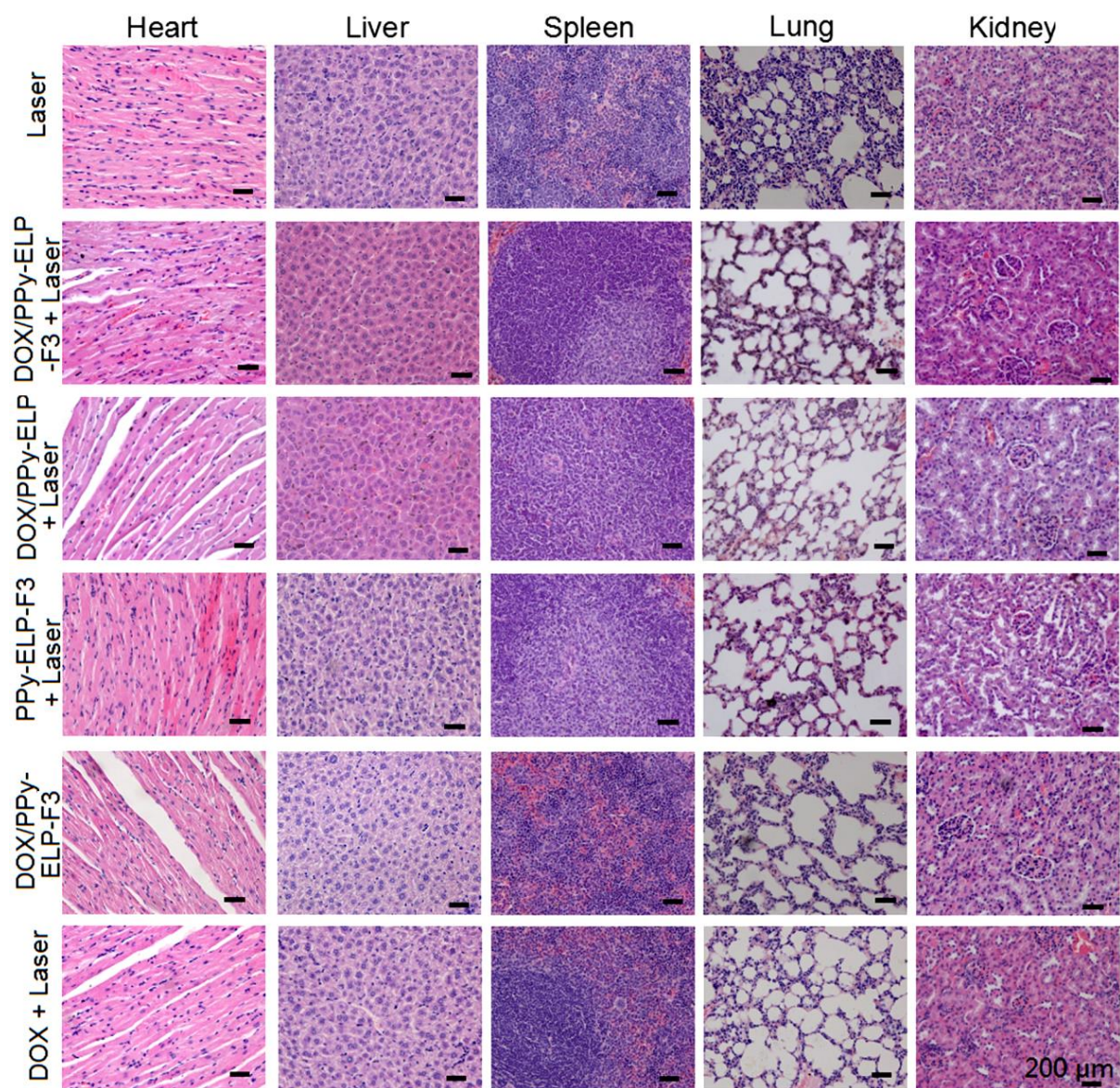


**Figure S24.** H&E staining of organs from different groups at 12 days post treatments.

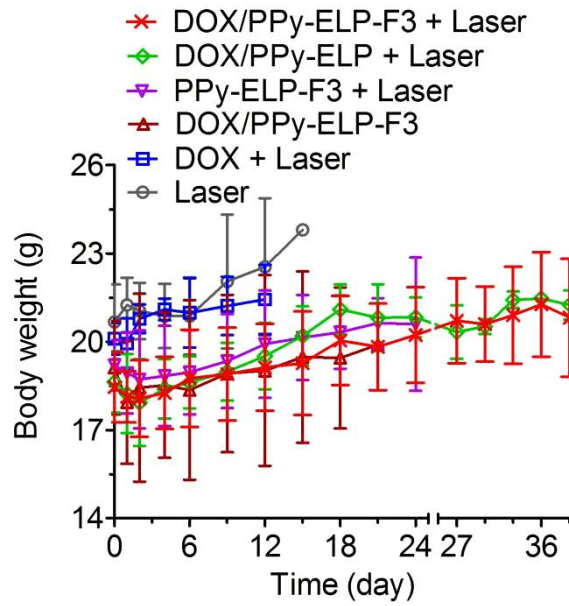


**Figure S25.** The change of body weights of mice in different groups after the treatments.

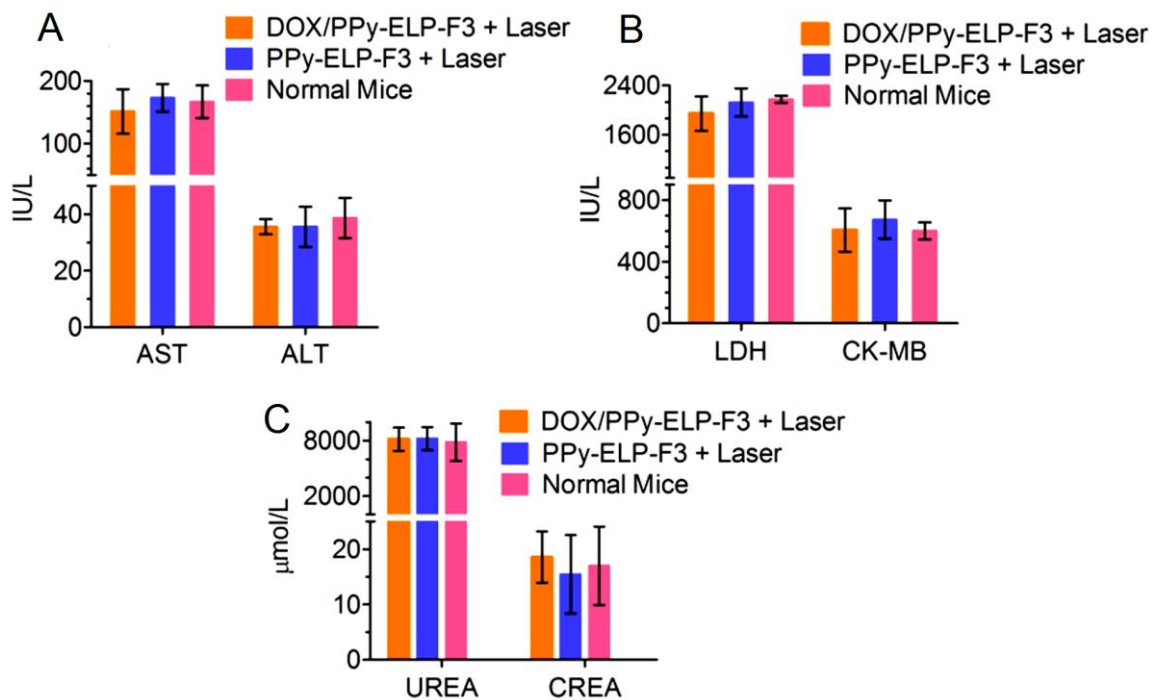


**Figure S26.** Clinical biochemistry parameters for mouse post administration compared with normal mice. Liver function markers (A): ALT, alanine aminotransferase; AST, aspartate aminotransferase. Heart function markers (B): LDH, lactate dehydrogenase; CK-MB, creatine kinase isoenzymes. Kidney function markers (C): creatinine, CREA; UREA. Blood samples were collected at 12 days post different treatments.

**Table S1.** Zeta potentials of different samples in the same equivalent concentration of DOX (40 mg DOX/L and 200 mg PPy/L), dispersed in 50 mM PBS of pH 5.5 and pH 7.4.

pH	Zeta potential (mV)					
	PPy	PPy-MA	PPy-ELP-F3	DOX/PPy-ELP-F3	PPy-ELP	DOX/PPy-ELP
pH 7.4	-5.49 ± 0.23	-9.56 ± 0.23	-6.74 ± 0.59	-4.70 ± 0.57	-6.69 ± 0.34	-5.11 ± 0.21
pH 5.5	-4.65 ± 0.24	-8.88 ± 0.60	-5.62 ± 0.38	-4.28 ± 0.29	-6.02 ± 0.25	-5.09 ± 0.19

**Table S2.** Important kinetic parameters of DOX/PPy-ELP-F3, DOX/PPy-ELP and DOX in blood circulation (n = 3).

Parameters	DOX/PPy-ELP-F3	DOX/PPy-ELP	DOX
Terminal half-life t <sub>1/2β</sub> (h)	20.58 ± 2.19	20.63 ± 3.16	5.26 ± 1.07
Area under curve AUC(0-∞) (uM/L×h)	40.18 ± 5.17	42.37 ± 9.58	5.82 ± 1.76

**Table S3.** Serum biochemistry analysis of normal mice, mice treated with PPy-ELP-F3 plus laser and DOX/PPy-ELP-F3 plus laser. Blood samples were collected at 12 days post different treatments.

Group	DOX/PPy-ELP-F3 + laser	PPy-ELP-F3 + laser	Normal mice
WBC (×10 <sup>9</sup> /L)	20.03 ± 1.21	21.82 ± 4.13	24.31 ± 5.36
RBC (×10 <sup>12</sup> /L)	6.00 ± 0.27	6.10 ± 0.30	5.86 ± 0.44
HGB (g/L)	181.4 ± 8.5	178.5 ± 20.9	166.0 ± 17.4
HCT (%)	47.01 ± 1.18	31.22 ± 9.04	30.31 ± 6.05
MCV (fl)	39.24 ± 1.04	39.49 ± 0.85	39.28 ± 0.83
MCH (pg)	15.14 ± 0.10	15.13 ± 0.29	14.72 ± 0.56
MCHC (g/L)	385.7 ± 10.4	362.1 ± 12.3	348.7 ± 7.8
PLT (×10 <sup>9</sup> /L)	301.1 ± 27.5	319.4 ± 20.4	323.9 ± 24.1
RDW-CV (%)	20.04 ± 1.51	21.78 ± 3.25	20.34 ± 0.93
RDW-SD (fl)	28.17 ± 1.39	27.16 ± 2.41	26.12 ± 0.61
PDW (fl)	10.37 ± 1.39	10.21 ± 0.55	10.86 ± 1.15
MPV (fL)	8.03 ± 0.92	8.07 ± 0.50	8.30 ± 0.24
PCT (%)	0.36 ± 0.11	0.29 ± 0.17	0.40 ± 0.12
P-LCR (%)	15.57 ± 0.94	14.10 ± 2.70	15.39 ± 1.47